A Rectangular Double-Helix Receiver Coil for Wireless Charging of Drones

Uvir Gordhan
Department of Electrical Engineering
University of Cape Town
Cape Town, South Africa
grduvi001@myuct.ac.za

Sampath Jayalath
Department of Electrical Engineering
University of Cape Town
Cape Town, South Africa
sampath.jayalath@uct.ac.za

***Abstract*— Inductive Power Transfer (IPT) for drones is an efficient form of charging to increase functionality of the drone. The design of the magnetic coupler, specifically the receiving coil is important. This coil is placed on the drone and is required to be lightweight, have a strong coupling, high efficiency, and a high misalignment tolerance. A ferrite-less rectangular double-helix receiver coil is proposed with a planar rectangular transmitter to meet these requirements. The proposed coupler achieves a 0.27 coupling coefficient and coil-to-coil efficiency of 97.88% while charging a drone with a battery capacity of 10000mAh at a nominal voltage of 22.2V. The coupler has excellent misalignment tolerance both in the direction of the x and y-axis.**

Keywords—Inductive Power Transfer, double-helix, battery capacity, compensation network, resonant frequency, coupling coefficient, drones.

I. INTRODUCTION

Drones are used in a variety of applications such as surveillance, agriculture, inspection of power lines, aerial mapping, and courier services [1]. They are powered by batteries that generally have a low battery capacity. These batteries require frequent charging which means the drone needs to make a return flight to a base station to physically connect the battery to power. As a result, the range of operation of these vehicles as well as their flight time is limited [2]. Wireless charging provides a smart, convenient, and time efficient solution that can increase a drone's functionality.

Inductive Power Transfer (IPT) is the most commonly used technology for wireless power transfer in drones. An IPT system consists of input and output side power electronics circuits, and the coupler (transmitter (Tx) coil and receiver (Rx) coil). When designing a magnetic coupler for drone applications, the safety of the electronics systems on-board must be considered as the generated magnetic field from the coupler can cause electromagnetic interference and damage these systems. Another consideration should be the misalignment between the Tx and Rx coils. This decreases the performance of power transfer and contributes to leakage magnetic fields. The weight of the Rx coil needs to be kept at a minimum to reduce the overall weight of the drone's payload. In summary, an IPT system for a drone should have a strong coupling, low leakage magnetic field, high tolerance to misalignment and should be as light as possible.

This paper focuses on the area of coupler designing and emphasizes the design of the Rx coil. The placement and shape of the Rx coil are dependent on the type of drone and its landing gears while the Tx coil must be designed to achieve maximum coupling with the Rx coil. **Fig. 1** illustrates the different types of landing gear that are common for drones. In addition, some drones do not have landing gears, and planar coils are used for the Rx coil in such drones [3],[4]. Song. et al proposed three single solenoid receivers for the three legs of the tripod-shaped landing gear [5]. Ke. et al and Campi. et al proposed a Rx coil for small-legged landing gear in which the coil is wound around the four legs [6], [7]. Cai. et al proposed a Rx coil for the U-shaped landing gear [8]. The T-shaped landing gear is common among many modern drones, and there are hardly any Rx coils proposed for it. The structure of the T-shaped landing gear allows for a solenoid or flux pipe Rx coil. One of the major drawbacks of these coils is that they only couple parallel magnetic fluxes, which means they can only couple with a transmitter that generates a parallel magnetic flux. The DDP, DDQP or BPP coils are most commonly used for this purpose. However, DDQP and BBP coils require complex power electronics systems which is a disadvantage. Therefore, this paper proposed a rectangular double-helix coil that is capable of coupling perpendicular flux to achieve higher coupling with a rectangular transmitter coil. Additionally, the performances of the proposed coupler are compared with solenoid-solenoid and solenoid-DDP as they are viable solutions for the T-shaped landing gear.

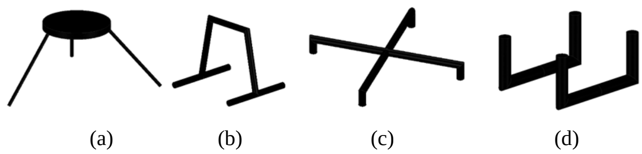

Fig. 1. Landing gears: (a) tripod-shaped [5], (b) t-shaped, (c) small-legged [6],[7], (d). u-shaped [8].

II. DOUBLE-HELIX COIL

Double-helix coils are created by superimposing two windings concentrically with opposite tilt and current direction [9]. **Fig. 2** illustrates the inner and outer layer of the superimposed windings. When the windings are configured like so, the x-components of the magnetic field (solenoid field) cancel, and the y-components are summed to produce a pure dipole field. The strength of the dipole field depends on the angle of tilt. Strong dipole fields can be obtained with tilt angles ranging from 15-45 degrees. It is crucial that the spacing between windings, and the tilt angle is kept the same for the inner and outer layer of the double-helix coil. This is to ensure the cancellation of the solenoid magnetic field and the addition of the dipole magnetic field. [10].

III. DESIGN OF IPT SYSTEM

A typical IPT system for WPT of drones consists of the AC power source, a power factor correction (PFC) converter, an inverter, primary compensation circuit, magnetic coupler, secondary compensation circuit, a rectifier, and the drone battery. By identifying the battery specifications, the power electronics system and the magnetic coupler can be designed accordingly. The compensation topology and coil quality factors are discussed briefly. The method of determining system currents and voltages is provided in this section.

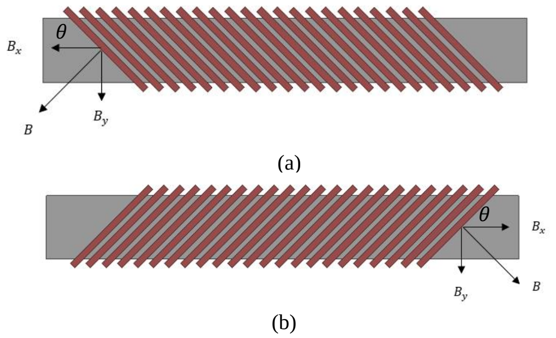

Fig. 2. Configuration of Double Helix Coil: (a). inner layer (b). outer layer

A. UAV Battery

The IPT system in this paper is required to charge a battery with a capacity of 10000mAh, a nominal voltage of 22.2V and a maximum charging voltage of 25.2V. The load can be equated to a resistor by determining the DC equivalent resistance of the battery ($V_{dc} = I_{dc}.R_{dc}$).

B. Compensation Topology

The function of the primary compensation is to minimize the input apparent power or to minimize the volt-ampere (VA) rating of the power supply. The secondary compensation maximizes the power transfer capability [11]. There are four basic compensation topologies: Series-Series (SS), Series-Parallel (SP), Parallel-Series (PS) and Parallel-Parallel (PP). SS and SP compensation topologies are implemented the most as they have higher efficiencies. These topologies can provide a constant voltage and constant current output which is required for battery charging. The SS topology is independent of the coupling coefficient. Furthermore, the output current of an SS compensated circuit is independent of the load. The SS topology also exhibits a lower sensitivity to misalignment when compared to the SP topology [12]. Hence, the SS compensation is adopted for this paper.

TABLE I. SYSTEM PARAMETERS

System Parameters		
Parameter	***Symbol***	***Value***
Inverter Output Voltage	V_{Speak}	$66.71V$
Resonant Frequency	f_0	$60kHz$
Primary Self-Inductance	L_1	$94.48\mu H$
Secondary Self-Inductance	L_2	$18.03\mu H$
Mutual Inductance	M	$11.25\mu H$
Coupling Coefficient	k_0	0.27
Primary Compensation Capacitor	C_1	$74.47nF$
Secondary Compensation Capacitor	C_2	$390.25nF$
Primary Peak Current	I_{1peak}	$7.56A$
Secondary Peak Current	I_{2peak}	$15.73A$
Primary Coil Resistance	R_1	$39.75m\Omega$
Secondary Coil Resistance	R_2	$33.79m\Omega$
Equivalent Resistance of Battery	R_{Lac}	2.04Ω

C. Quality of the Coils

The maximum power transfer efficiency for an IPT system with SS compensation topology is given by [13]:

$$\eta = \frac{k^2 Q_1 Q_2}{\left(1+\sqrt{1+k^2 Q_1 Q_2}\right)^2} \quad (1)$$

The maximum PTE is determined by the product of k^2 and the coil Q factors where $Q_1 = \omega_0 L_1/R_1$ and $Q_2 = \omega_0 L_2/R_2$ are the quality factors of the Tx and Rx coils respectively. To ensure stable power transmission the bifurcation phenomenon needs to be avoided. To meet this condition, the external quality factor should be considered. This is defined as [14]:

$$Q_e = \frac{\omega_0 L_2}{R_{eq}} \quad (2)$$

By ensuring that the coupling coefficient k_0 is less than the critical coupling k_c, bifurcation can be avoided [14]:

$$k_0 \ll k_c \approx \frac{1}{Q_e} \quad (3)$$

D. System Parameters

The system parameters for the IPT system are summarized in **Table I**. The primary and secondary currents and voltages of an SS compensated IPT system are defined below. To obtain resonance condition of the magnetic

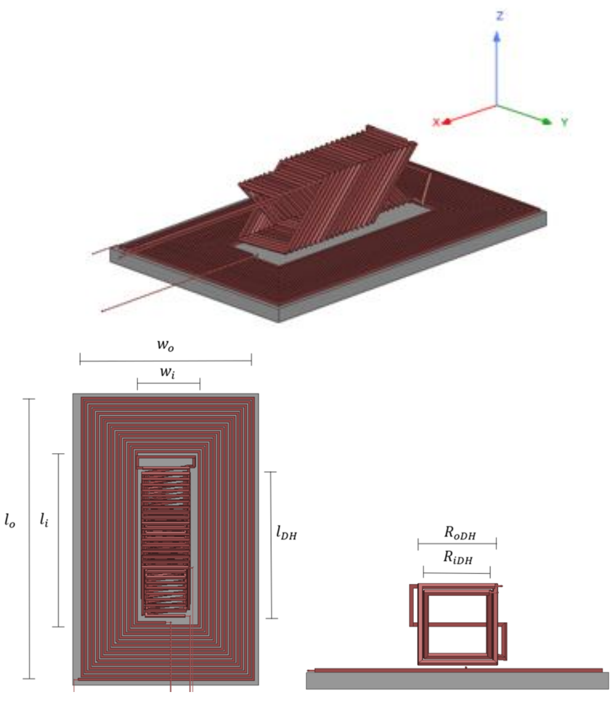

Fig.3. Simulated Rectangular Double-Helix Receiver with Planar Rectangular Transmitter

coupler, the value of the compensation capacitors need to be chosen appropriately. To determine these values, the lumped inductances (L_1, L_2 and M) are required. These are extracted from ANSYS Maxwell3D. The resonating capacitors can be calculated as follows [15]:

$$C_1 = \frac{1}{\omega_0^2 L_1} \tag{4}$$

$$C_2 = \frac{1}{\omega_0^2 L_2} \tag{5}$$

The approximated AC equivalent resistance of the load is given by [15]:

$$R_{Lac} = \frac{8}{\pi^2}(R_{Ldc}) \tag{6}$$

The peak current and voltage at the load are determined by calculating the equivalent AC values [15]:

$$V_{Lpeak} = V_{2peak} = \left(\frac{4}{\pi}\right)(V_{dc}) \tag{7}$$

$$I_{Lpeak} = I_{2peak} = \frac{V_{Lpeak}}{R_{Lac}} \tag{8}$$

Lastly, the supply voltage that is needed to achieve the load requirements as well as the peak current in the primary coil is calculated by determining the impedance as seen by the source [15].

$$V_{Speak} = I_{2peak}\omega_0 M \tag{9}$$

$$Z = \frac{\omega_0^2 M^2}{R_{Lac}} \tag{10}$$

$$I_{1peak} = \frac{V_{Speak}}{Z_{SP}} \tag{11}$$

TABLE II. COUPLER SPECIFICATIONS

Coil	**Dimensions of Coupler**	
	Dimension	***Value***
Double-Helix	Length (l_{DH})	150mm
	Inner Loop Radius (R_{iDH})	30mm
	Outer Loop Radius (R_{oDH})	40mm
Planar Rect.	Outer Length (l_o)	282mm
	Outer Width (w_o)	170mm
	Inner Length (l_i)	167mm
	Inner Width (w_i)	60mm

IV. RESULTS

A. System Analysis

The double-helix receiver and planar rectangular transmitter was analyzed using finite element analysis (FEA) software ANSYS Maxwell3D. The coupler was designed to charge a 10000mAh battery with a nominal voltage of 22.2V and maximum charging voltage of 25.2V. The IPT system was designed to charge at 25.2V. The equivalent diameter of copper wire that was used in simulations is 2.3mm to handle the peak currents produced by the system. The dimensions of the double-helix receiver and planar rectangular transmitter are provided in **Table II**. The magnetic coupler is illustrated in **Fig. 3**. The double-helix was designed with 20 turns on the inner loop and 20 turns on the outer loop. The transmitter has 16 turns and uses 3C90 ferromagnetic material [16]. The inductances and coupling coefficient of the magnetic coupler were extracted from Maxwell3D and the resonant frequency chosen for the IPT system is 60kHz. This satisfies equation (2) and maintains an external quality factor of 3.33. By referring to equation (3), the coupling coefficient of the magnetic coupler is kept below the critical coupling ensuring that bifurcation is avoided.

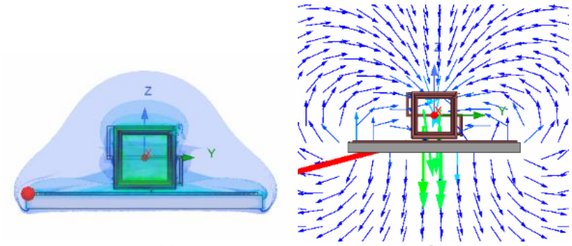

(a) (b)

Fig.4. Magnetic Field: (a). Field Distribution, (b). Field Vector

B. Magnetic Field Analysis

The magnetic field distribution and magnetic field vector for the nominal position of the magnetic coupler is illustrated in **Fig. 4**. The maximum limit defined by the ICNIRP on the magnetic field exposure allowed for humans is $27\mu T$ [17]. Hence, it is vital that the magnetic field of the coupler does not exceed $27\mu T$ beyond a reasonable distance. By referring to the magnetic field vector, the pure dipole field of the double-helix can be seen. This emphasizes the ability of a double-helix coil having a strong coupling capability with the perpendicular component of magnetic flux. Furthermore, the magnetic field reaches $27\ \mu T$ at 230mm in the z-axis,

TABLE III. COMPARISON OF MAGNETIC COUPLERS

Comparison of Couplers		
Coupler	***Coupling k***	***Weight (g)***
Solenoid - Solenoid	0.09	168.15
Solenoid - DD	0.16	168.15
Double-Helix – Rect. Planar	0.27	370.08

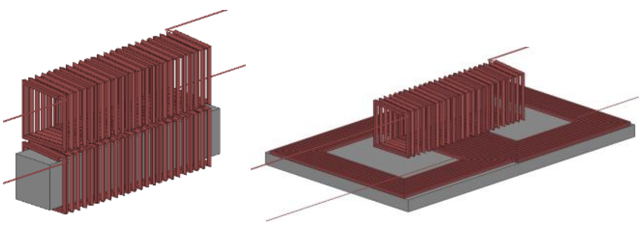

(a) (b)

Fig.5. IPT couplers (a). Solenoid-Solenoid (b). Solenoid-DD

approximately 20mm below the body of the drone considered in this study.

C. Coupler Efficiency

Equation (1) defines the maximum PTE for a coupler but assumes that the losses in ferrite are small compared to the winding losses [18]. However, to accurately calculate the coil-to-coil efficiency of the coupler, the power loss due to ferrite core material must be considered. Equations (12) and (13) are used to calculate the coil-to-coil efficiency and includes the core loss.

$$\eta = \frac{P_{out}}{P_{in}} \quad (12)$$

$$P_{out} = P_{in} - P_{core} - P_{winding} \quad (13)$$

Using equation (12) and (13) and the system parameters in **Table I**, the coil-to-coil efficiency was calculated as 97.88%.

D. Coupler Comparison

The performance of the proposed coupler was compared to two other couplers that could also be used for T-shaped landing gears. A solenoid receiver with a solenoid transmitter, and a solenoid receiver with a DD transmitter. For the comparison, the length and the inner radius of the solenoid receiver in both couplers is the same as the double-helix receiver. The length and width of the DD transmitter is the same as the rectangular planar transmitter. The transmission distance was also kept the same. These are illustrated in **Fig. 5**. For both couplers, the transmitter uses ferrite while the receiver uses no ferrite as in the proposed coupler. The weight of each Rx coil and the magnetic coupling for each coupler at nominal position is tabulated in **Table III**. Although, the weight of the solenoid receiver is less than the double-helix receiver, the coupling coefficient achieved with the double-helix coil is superior to the other two couplers. It can be seen that the ability of the double-helix to couple the perpendicular component of magnetic flux is advantageous in the context of drone charging.

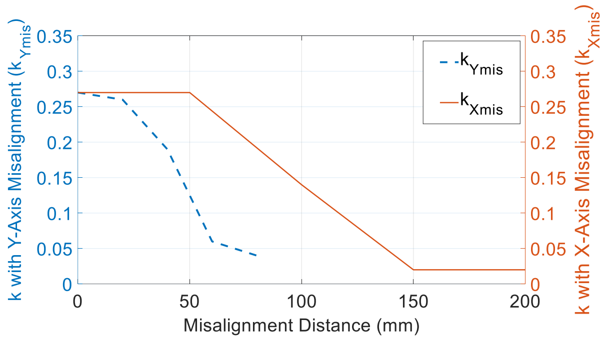

Fig.6. Coupling Coefficient vs *x* and *y*-axis Misalignment

E. Misalignment Analysis

The landing accuracy of drones is not considered in this paper as most drones have an internal navigation system or a GPS (Global Positioning System). However, a guiding system can be used to align the receiver and transmitter coils, as shown in [5].

The performance of the coupler with respect to misalignment between the receiver and transmitter was tested. **Fig.6** illustrates the change in the magnetic coupling coefficient with respect to x and y-axis misalignment. The misalignment parametric was run from the nominal position (0mm) to the point where the receiver is positioned at the edge of the transmitter. The y-axis misalignment parametric (k_{Ymis}) was run from 0mm-80mm and it can be seen that the coupling varies from 0.27 to 0.04. The x-axis misalignment parametric (k_{Xmis}) was run from 0mm-200mm and it is shown that the coupling varies from 0.27 to 0.02. At a y-axis misalignment of 45mm and an x-axis misalignment of 95mm the coupling coefficient of the proposed coupler decreases to 0.16. This is the maximum magnetic coupling achieved by the solenoid-DD coupler at nominal position with similar dimensions. This result further emphasizes the excellent performance of the proposed coupler. It was noted that the variation in the secondary inductance is 18.03-15.8 μH with the x-axis misalignment and almost constant with the y-axis misalignment. However, the primary inductance remains constant during x and y-axis misalignment.

V. Conclusion

This paper proposed a rectangular double-helix receiver that has high coupling and excellent misalignment performances. The high coupling of 0.27 was achieved without the use of ferrite core material on the receiver therefore minimizing the weight of the receiver coil. The coil-to-coil efficiency achieved is 97.88%. The IPT system with the proposed coupler avoids bifurcation, therefore, ensuring stable and efficient operation.

References

[1] Y. Song, X. Sun, H. Wang, W. Dong, Y. Ji, "Design of Charging Coil for Unmanned Aerial Vehicle-Enabled Wireless Power Transfer." *2018 8th Int. Conf. Power Energy Syst. (ICPES)*, 2018, pp. 268-272.

[2] C. Song, H, Kim, Y. Kim, D, Kim, S. Jeong, Y. Cho, S. Lee, S. Ahn, J.Kim, "EMI Reduction Methods in Wireless Power Transfer System for Drone Electrical Charger Using Tightly Coupled Three-Phase Resonant Magnetic Field", *IEEE Trans. Ind. Electron*, vol. 65, no. 9, pp. 6839-6849, 2018.

[3] J. Zhou, B. Zhang, W. Xiao, D. Qiu, and Y. Chen, "Nonlinear parity-time-symmetric model for constant efficiency wireless power transfer: Application to a drone-in-flight wireless charging platform," *IEEE Trans. Ind. Electron*, vol. 66, no. 5, pp. 4097–4107, 2019.

[4] C. Cai, J. Wang, H. Nie, P. Zhang, Z. Lin, and Y.-G. Zhou, "Effective-configuration WPT systems for drones charging area extension featuring quasi-uniform magnetic coupling," *IEEE Trans. Transp. Electrific.*, vol. 6, no. 3, pp. 920–934, 2020.

[5] C. Song, H. Kim, Y. Kim, D. Kim, S. Jeong, Y. Cho, S. Lee, S. Ahn, and J. Kim, "EMI reduction methods in wireless power transfer system for drone electrical charger using tightly coupled three-phase resonant magnetic field," *IEEE Trans. Ind. Electron*, vol. 65, no. 9, pp. 6839–6849, 2018.

[6] D. Ke, C. Liu, C. Jiang, and F. Zhao, "Design of an effective wireless air charging system for electric unmanned aerial vehicles," in *Proc. 43rd Annu. Conf. IEEE Ind. Electron. Soc.*, Oct. 2017, pp. 1–4.

[7] T. Campi, S. Cruciani, F. Maradei, and M. Feliziani, "Wireless charging system integrated in a small unmanned aerial vehicle (UAV) with high tolerance to planar coil misalignment," in *Proc. EMC Sapporo/APEMC*, Sapporo, Japan, 2019, pp. 601–604.

[8] C. Cai, J. Liu, S. Wu, Y. Zhang, L. Jiang, Z. Zhang, and J. Yu, "Development of a cross-type magnetic coupler for unmanned aerial vehicle IPT Charging Systems," *IEEE Access*, vol. 8, pp. 67974–67989, 2020.

[9] R. B. Meinkeo, M. J. Ball, and C. L. Goodzeit, “Superconducting double-helix accelerator magnets,” in *Proc. Part. Accel. Conf*., vol. 3, May 2003, pp. 1996–1998.

[10] C. Goodzeit, M. Ball and R. Meinke, "The double-helix dipole-a novel approach to accelerator magnet design", *IEEE Trans. Appl. Supercond.*, vol. 13, no. 2, pp. 1365-1368, 2003. Available: 10.1109/tasc.2003.812672.

[11] W. Zhang and C. Mi, "Compensation Topologies of High-Power Wireless Power Transfer Systems", *IEEE Trans. Veh. Technol*, vol. 65, no. 6, pp. 4768-4778, 2016.

[12] V. Shevchenko, O. Husev, R. Strzelecki, B. Pakhaliuk, N. Poliakov and N. Strzelecka, "Compensation Topologies in IPT Systems: Standards, Requirements, Classification, Analysis, Comparison and Application", *IEEE Access*, vol. 7, pp. 120559-120580, 2019.

[13] S. Jayalath and A. Khan, “Design, challenges, and trends of inductive power transfer couplers for electric vehicles: A Review,” *IEEE J. Emerg. Sel. Topics Power Electron*., vol. 9, no. 5, pp. 6196–6218, 2021.

[14] H. Kim, C. Song, D.-H. Kim, D. H. Jung, I.-M. Kim, Y.-I. Kim, J. Kim, S. Ahn, and J. Kim, “Coil design and measurements of automotive magnetic resonant wireless charging system for high-efficiency and low magnetic field leakage,” *IEEE Trans.Microw. Theory Techn.*, pp. 1–18, 2016

[15] K. Woronowicz, A. Safaee and T. Dickson, "Single-Phase Zero Reactive Power Wireless Power Transfer Topologies Based on Boucherot Bridge Circuit Concept", *Can. J. Electr. Comput. Eng*,, vol. 38, no. 4, pp. 323-337, 2015. Available: 10.1109/cjece.2015.2468057.

[16] S. Bandyopadhyay, P. Venugopal, J. Dong, and P. Bauer, “Comparison of magnetic couplers for IPT-based EV charging using multi-objective optimization,” *IEEE Trans. Veh. Technol*, vol. 68, no. 6, pp. 5416–5429, 2019.

[17] F. Lin, A. Zaheer, M. Budhia and G. Covic, "Reducing Leakage Flux in IPT Systems by Modifying Pad Ferrite Structures", in *Proc. IEEE Energy Convers. Congress Exp*o, Pittsburgh, PA, USA, 2014, pp. 1770-1777.

[18] R. Bosshard, J. W. Kolar, J. Muhlethaler, I. Stevanovic, B. Wunsch, and F. Canales, “Modeling and - -pareto optimization of inductive power transfer coils for electric vehicles,” *IEEE J. Emerg. Sel. Topics Power Electron*., vol. 3, no. 1, pp. 50–64, 2015.